Vehicle System Dynamics
2011, 1–14, iFirst

Measuring sideslip and camber characteristics of bicycle tyres

Andrew Dressel* and Adeeb Rahman

Civil Engineering and Mechanics, University of Wisconsin-Milwaukee, PO Box 784, Milwaukee, WI 53201, USA

(*Received 1 February 2011; final version received 14 August 2011*)

Sideslip and camber tyre properties, the forces and moments a tyre generates as it rolls forward under different circumstances, have been found to be important to motorcycle dynamics. A similar situation may be expected to exist for bicycles, but limited bicycle tyre data and a lack of the tools necessary to measure it may contribute to its absence in bicycle dynamics analyses. Measuring these properties requires holding the tyre at a fixed orientation with respect to the pavement and its direction of travel, and then measuring the lateral force and torque about the steer axis generated as the tyre rolls forward. Devices exist for measuring these characteristics of automobile tyres. One device is known to exist specifically for motorcycle tyres, and it has been used at least once on bicycle tyres, but the minimum load it can apply is nearly double the actual load carried by most bicycle tyres. This paper presents a low-cost device that measures bicycle tyre cornering stiffness and camber stiffness.

Keywords: bicycle; characteristic; tyre; property; measurement

1. Introduction

Sideslip and camber tyre properties, specifically the forces and moments a tyre generates as it rolls forward under different circumstances, have been found to be important to motorcycle dynamics [1,2]. A similar situation may be expected to exist for bicycles, but limited and conflicting bicycle tyre data and a lack of the tools necessary to measure them may contribute to their absence from bicycle dynamics analyses [3,4]. This paper describes tools developed to measure these bicycle tyre properties and presents some of the findings (Figure 1).

2. Motivations

Kooijman *et al*. [5] found tyre properties to be insignificant on bicycles at speeds below 6 m/s by physical experimentation. On the other hand, cornering stiffness, also known as sideslip and lateral slip stiffness, of either the front or rear tyres, has been found to influence both the weave and wobble modes of motorcycles. [1] We wondered if bicycle tyre properties matter

*Corresponding author. Email: adressel@uwm.edu

ISSN 0042-3114 print/ISSN 1744-5159 online

DOI: 10.1080/00423114.2011.615408
http://www.informaworld.com

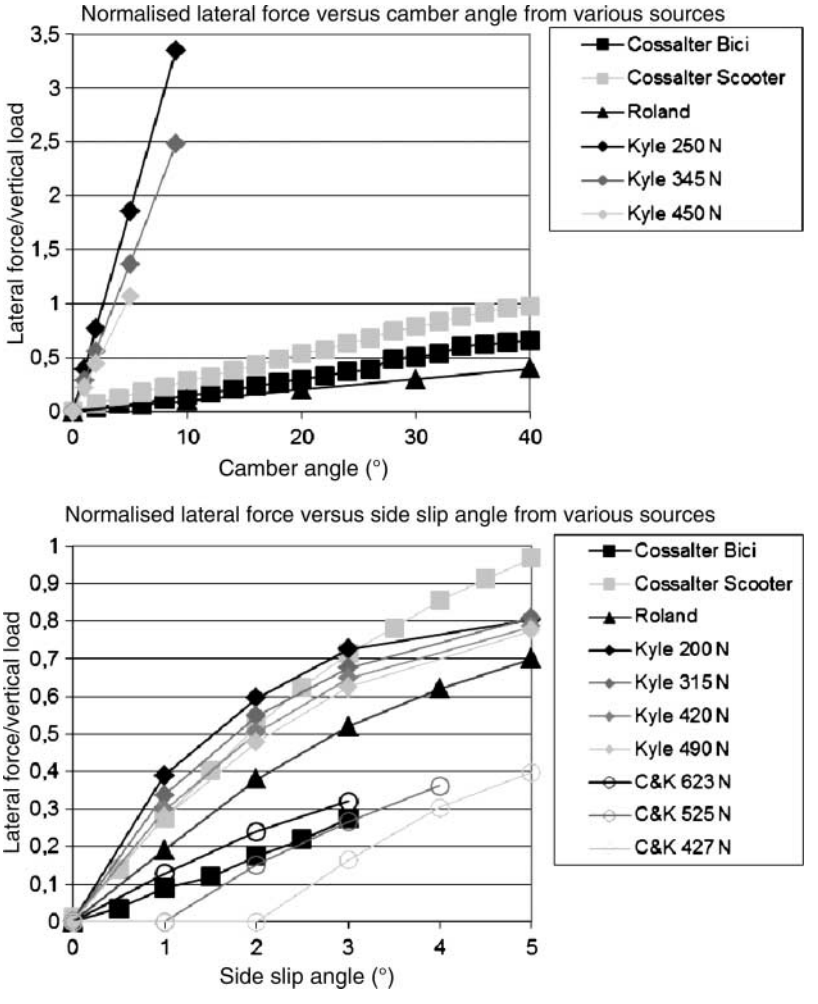

Figure 1. Bicycle tyre and scooter tyre sideslip, and camber properties data reported by Cossalter, Roland, Kyle, and Cole and Khoo.

at higher speeds, and we started by looking for the influence of tyres on the wobble mode for bicycles in numerical simulations.

To perform the simulations, we first entered the geometry and mass distribution described by Meijaard *et al*. [6] in their benchmark paper into the FastBike numerical simulation described by Cossalter *et al*. [7]. We set the suspension to be fixed and the tyre properties to be as close as possible without causing numerical difficulties to rigid, knife-edge wheels that roll without slip. We calculated stability eigenvalues in FastBike and exported them in the maximum precision available, two decimal places. Ignoring additional values caused by the additional degrees of freedom, we found the remaining eigenvalues to agree with the published results, validated by Kooijman *et al*. [5], to within the available precision (Figure 2).

We then used this validated bicycle model in FastBike to gauge its sensitivity to sideslip and camber tyre properties. To specify bicycle tyres, we started with the stock motorcycle tyre properties provided with FastBike and modified them to incorporate the dimensions described by Kooijman *et al*. [5], 'New standard road tyres, 28×1 3/8 (Halfords brand)': ETRTO 37-622. We then used the limited bicycle tyre sideslip and camber properties described

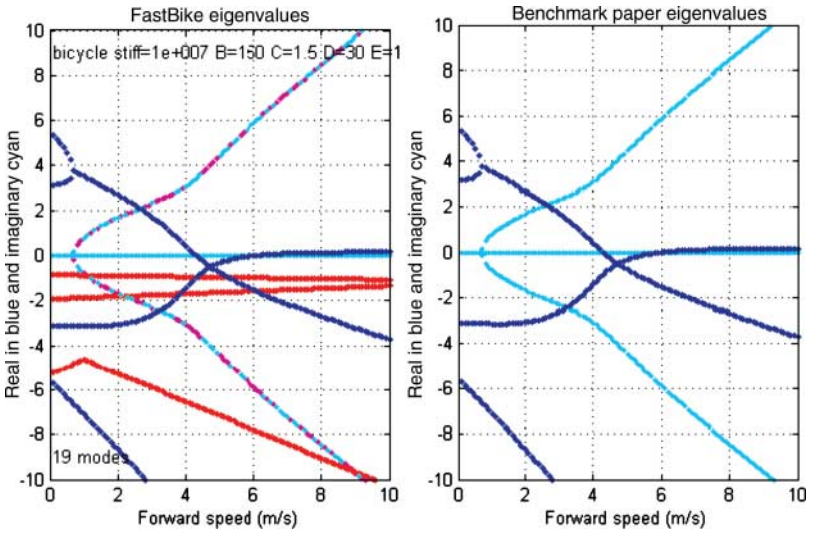

Figure 2. Stability eigenvalues from FastBike and the Benchmark Paper.

by Cossalter [1] to generate new Magic Formula coefficients [2], as required by FastBike. Relaxation length is computed internally by FastBike from cornering stiffness and lateral stiffness and then incorporated via the carcass compliance and damping without additional relaxation equations [7].

We also incorporated the bicycle front fork flexibility data by Rinard [8] and the bicycle wheel flexibility data by Trovati [9] that we found online into the model to increase fidelity.

Through brief trial and error, we selected a combination of fork and wheel stiffnesses that, along with the combined tyre properties, produced a barely stable wobble mode. Then we altered the tyre cornering stiffness by $\pm 10\%$ to find that it would indeed cause the wobble mode to become unstable. We took this to mean that physically measuring the sideslip and camber properties of bicycle tyres might prove worthwhile (Figure 3).

There is not much funding available for bicycle research, however, and so we needed a cost-effective way to measure these tyre properties.

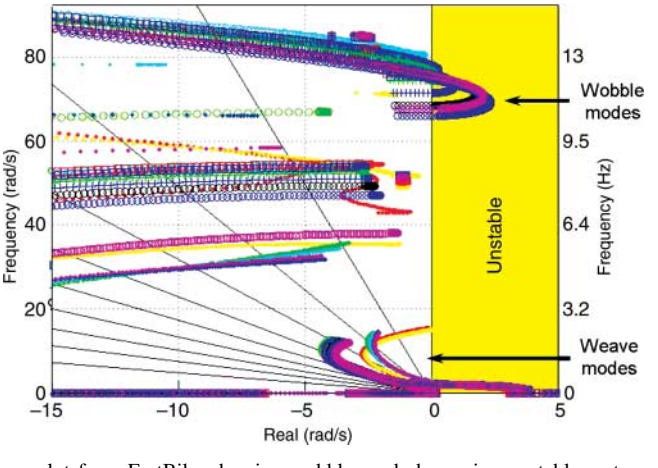

Figure 3. Root-locus plot from FastBike showing wobble mode becoming unstable as tyre cornering stiffness varies.

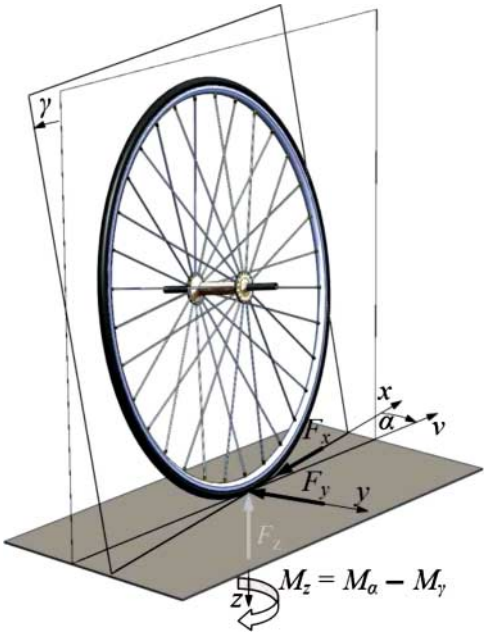

Figure 4. Slip angle α, camber angle γ, lateral force F_y, normal force F_z, and moments M_z acting on tyre to be measured.

3. Methodologies

Measuring these sideslip and camber tyre properties requires holding a tyre at a fixed orientation, camber angle γ, and steer angle δ, with respect to the pavement and its direction of travel, and then measuring the lateral force F_y and moment M_z acting on the tyre as it rolls forward. Several methods are described inside [1,2,10] and outside the literature [11,12]. We chose to collect data on an in-door, purpose-built, stationary, straight track because we thought it would be easier to control at a lower cost. We also chose to test one tyre at a time to avoid possible issues caused by variations from tyre to tyre. Our general design to accomplish this consists of a small cart that holds a bicycle wheel in the desired orientation, allows it to roll forward on the track, applies a vertical load, and measures the lateral force that builds up between the tyre contact patch and a fixed vertical surface, which enforces the direction of travel and causes the tyre to experience a slip angle α equal in magnitude to the input steer angle δ (Figure 4).

3.1. *The cart*

The cart is assembled predominantly from common dimensional lumber, mostly 2×4s, joined with various bolts and screws. This affords very quick and inexpensive construction and easy modification (Figure 5).

It consists of five main moving parts:

(1) A cart body that provides sufficient width to enforce a camber angle, sufficient length to enforce a steer angle, and a place to mount the other moving parts and electronic equipment. It is supported by the bicycle wheel on the front side and two swivel casters mounted to the bottom of the cart near the back edge.
(2) A yoke that pivots on door hinges with respect to the cart body about a longitudinal axis nearly through the contact patch to enable setting the camber angle, while moving the

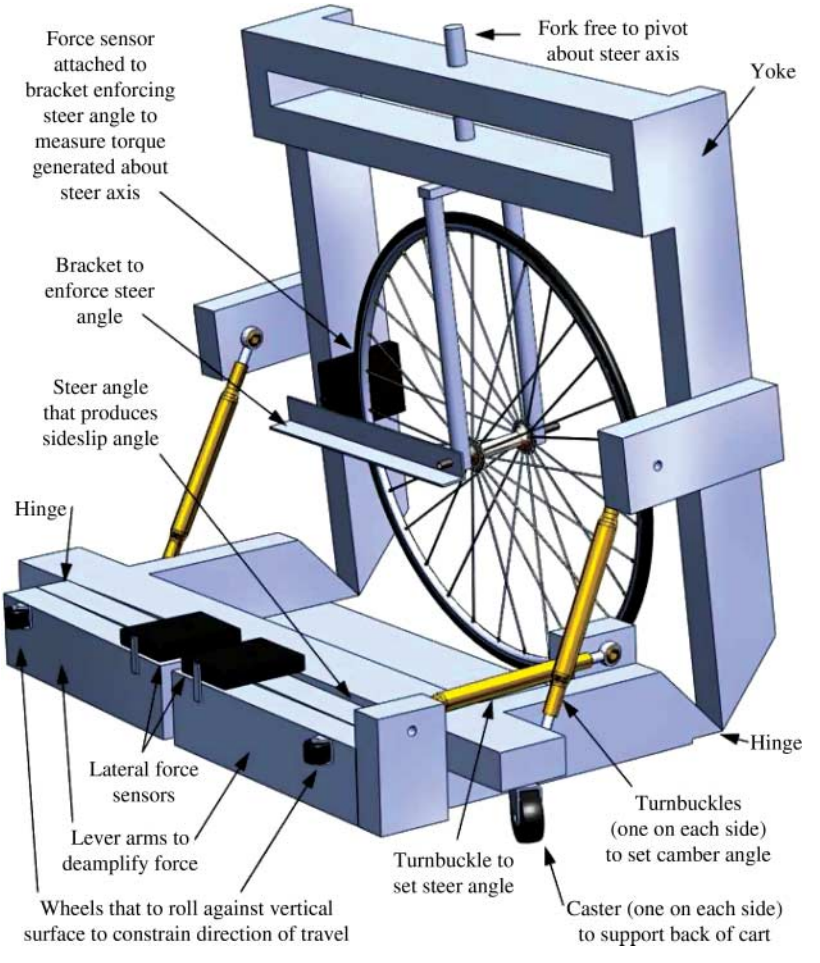

Figure 5. The test cart.

contact patch laterally and tilting the cart only by a minimal amount. The desired camber angle is set and held with two rigid turnbuckles sold for use as the top links in three-point hitches for attaching implements to small farm tractors.

(3) A fork that pivots freely with respect to the yoke about a steering axis through the contact patch, but that is held fixed by a force sensor to measure torque generated in the contact patch about that steer axis.

(4) A steering board that attaches to the cart body on the back side, opposite to the bicycle wheel, with a hinge on one end and a third turn buckle on the other, so that it can be held at a fixed steer angle with respect to the cart body and the bicycle wheel.

(5) A pair of lever arms that pivot on hinges mounted to the back side of the steering board to deamplify the lateral force generated, so that the force sensors are not saturated. A fixed caster is mounted on the rear of each lever arm to roll along a straight vertical surface fixed to the track and thus enforce the wheel direction of travel.

It was understood that the frame would have some finite flexibility, but it was thought that a final lateral force value could be read after any slack was taken up. In hindsight, this flexibility makes establishing a measurable tyre orientation problematic, and

Figure 6. Mechanism to enforce wheel orientation and measure torque generated about the steering axis.

it may contribute to the discrepancy we observed between calculating the relaxation length as the ratio of the cornering stiffness over the lateral stiffness and calculating the relaxation length as the distance travelled before the lateral force reaches 63% of its stead-state value.

Although steer and camber angles must be measured separately, they can be set precisely and finely with the turnbuckles in any combination The orientation of the tyre is additionally enforced and the wheel flex minimised by two sets of guide wheels that run on the braking surface of the bicycle rim. One is at the bottom of the wheel, near the contact patch, to prevent flexing due to the lateral force generated at the contact patch. The second is at the front of the wheel to prevent rotation about the steering axis due to torque generated at the contact patch. This minimises the changes in the steering angle caused by flexing of the force sensor or the wheel (Figure 6).

The desired vertical load on the tyre is generated by appropriately sized steel blocks simply clamped to the frame near the contact patch to maximise the load borne by the tyre and to minimise the load on the casters. Loads of 22.5 and 45 kg were used.

3.1.1. *Data collection*

Nearly any sufficiently accurate force measuring system may be used to detect the generated lateral force, and this implementation uses a system from PASCO® intended for classroom experiments [13]. The individual force sensors, described by PASCO® as having a 1% accuracy, 0.03 N resolution, and up to a 1000 Hz sample rate, are rated for only ± 50 N. This is far less than the maximum expected lateral force from the tyre, and so a simple lever mechanism, similar to the one PASCO® uses on their stress–strain apparatus, is employed to scale down by five to one the expected lateral force generated by the tyre, well below the 50 N maximum. The force sensors 'employ four strain gauges epoxied to a binocular dual beam made from annealed aluminium. The strain gauges are wired to form a full-bridge circuit that is driven by a constant voltage source. The voltage across the bridge circuit is proportional to the applied force'. In total, three force sensors are used: two to measure the lateral force while also maintaining the cart and wheel steer angle, and one to measure torque.

We calibrated the values from the two lateral force sensors against the actual force generated in the tyre contact patch by suspending the cart from a vertical cable just enough for the bottom of the tyre to clear the ground, and then pushing against it with a third force sensor. The ratio between the sum of the first two with the third is used to convert recorded data into lateral force values.

A fourth sensor which measures rotary motion, records the horizontal distance moved. The PASCO® system enables recording all these values together along with the time at which they are collected.

3.1.2. *Orientation measurement*

There are no gauges or indicators on the cart to show the actual tyre orientation. Instead we calculate it from four measurements between the vertical track and the braking surface of the rim: at the top, bottom, front edge, and rear edge. Once we found the wall to be unsuitable for the vertical track and selected an extruded aluminium track instead, we no longer had a vertical surface to measure against. Instead we constructed a jig out of extruded aluminium bars that provided four properly located points to which we could measure the distance from four points on the wheel. We placed the jig on the track to measure the orientation whenever we changed it, and removed the jig in order to roll the cart forward to measure the tyre sideslip and camber properties. See point 2 in Section 3.3 for more details.

3.2. *The track*

We chose a flat and straight track, instead of a drum or disk to avoid issues created by either vertical or horizontal curvature, such as those described by Cossalter [1]. Although, we initially thought that we could take advantage of any sufficiently long, level, rigid, and smooth stretch of floor adjacent to a plumb, straight, rigid, and smooth wall to provide the test track, we were unable to find such a suitable combination. The recorded lateral force data were very noisy and it was difficult to pick a single value from them. Instead, we built several special tracks on which we could test.

We were confident in the straightness of our vertical track because it was a 15 cm deep piece of extruded aluminium.

In an effort to eliminate issues of measuring flatness and levelness, we turned to the self-levelling compound, a highly plasticised quick-curing concrete poured onto a 3 m long, 1 m tall, and 30 cm wide steel I-beam laid on its side. To ensure a quality bond, we treated the steel with a bonding agent and attached a thin steel mesh about 3 mm off the surface with epoxy. We added a retardant to the compound to give it time to flow and we added a mechanical shaker to the I-beam web to induce flowing.

In all cases, the necessary coefficient of friction between the track and the tyre is provided by the anti-skid tape: approximately 80-grit sandpaper (Figure 7).

3.2.1. *Vertical load measurement*

Because of the geometry of the cart and how it changes to accommodate changes in the steer or the camber angle, the vertical load must be measured after any change in the steer or the camber angle and before any data collection. This is accomplished with an antique, but perfectly functioning balance scale set even with the end of the track. The cart is simply rolled so that only the bicycle tyre rests on the scale and its weight is recorded.

Figure 7. The test device on its final track: the self-levelling compound poured on the web of a large steel I-beam. The black strip of anti-skid tape can be seen along the right edge and the extruded aluminium strip along the left edge.

3.2.2. *Cart towing*

We wanted to tow the cart forward at a consistent speed to produce the best results. At first, we merely pulled by hand on a cord attached to the front of the cart. We quickly replaced that with a crank set cut out of a bicycle frame and a chain attached to the front of the cart. Finally, we stumbled upon a scrap piece of soil testing equipment that had a working electric motor, three-speed gear box, and an external half-inch (12.7 mm) pitch chain drive. It fitted at the end of the track perfectly and provided a wonderfully consistent towing force (Figure 8).

The lateral force generated by the tyre is transitory and dissipates quickly once the tyre stops rolling: by about 0.05 N per second per sensor, and this dissipation is also observed when measuring the static lateral stiffness of the tyres. This suggests that the tyre needs to be rolled forward at a sufficient speed, but forward speed also adds noise to the recorded data as the cart jostles due to imperfections in the contacting surfaces. To minimise both the force dissipation and the noise, we increased the forward speed until we found no change in the lateral force with speed, and then used the slowest speed that produced that force. Data recorded from high-speed runs are labelled ‘fast’ in Figure 11.

Measurement of a known constant force, a simple weight, with the PASCO® force sensors was not found to vary noticeably with time, and so we believe that it is the force generated by the tyre that dissipates with time.

Figure 8. Cart towing device.

3.3. *Testing protocol*

Recording quality data with this apparatus requires a strict protocol:

(1) Tyre pressure. Inflate to target value and record.
(2) Orientation. Set the measuring jig on the track around the cart. Make sure it is firmly up against the vertical track and the two end uprights are vertical with a spirit level. Measure the perpendicular distance from the inside edge of it to the wheel rim at the top, bottom, and left and right extremes. Enter these values into a spreadsheet to calculate the wheel orientation in degrees. Adjust turnbuckles as necessary to produce the desired camber and/or the steer angle. Remove the jig and tow the cart forward under simulated test conditions. Stop half way down the track. Replace jig and measure orientation under the near-target lateral force and steer torque.
(3) Vertical load. Put the scale and a wooden ramp at the end of the track, and roll the test cart onto the scale. Record the vertical load.
(4) Move the cart back onto the track; make sure it is just barely up against the vertical track to enforce the desired steer angle.
(5) Momentarily hold the contact points away from the force sensors and zero them.
(6) Attach the tow chain, start recording data, and turn on the electric tow motor.
(7) At the end of the track, the advancing cart automatically turns off the electric motor, and data recording stops automatically at 1.5 m.
(8) Disengage the tow chain from its sprocket and roll the cart back to the start, reorient the cart, re-zero the sensors, and return to Step 6. Repeat for several runs.
(9) Export data from the PASCO® software. Import it into MATLAB®. Check for repeatability of average lateral force value: standard deviation of the averages < 0.20 and standard deviation of each run < 0.5. If good, record average value and return to Step 2. If not, return to Step 6.

3.4. *Data processing*

Several runs are performed at each orientation until a desired level or repeatability is reached. Outliers are rejected, and the final recorded value for that camber and steer angle is the average of the closest cluster of values (Figure 9).

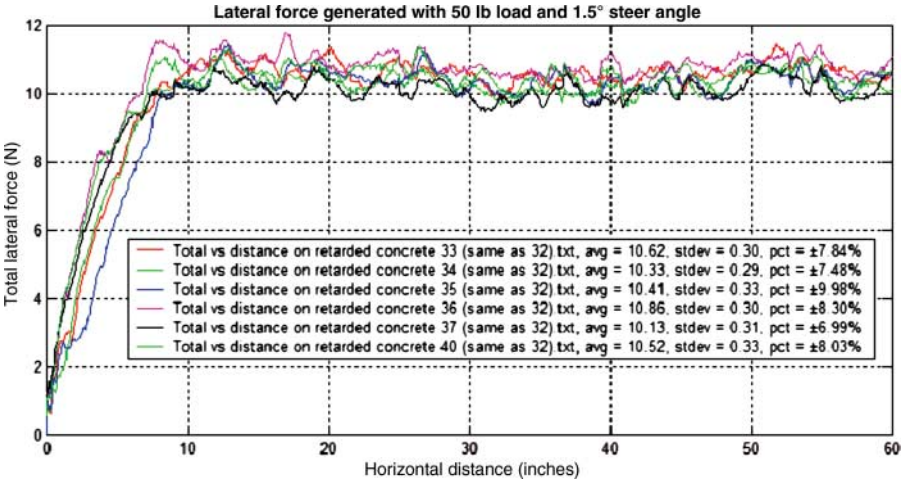

Figure 9. Raw test data from six consecutive runs.

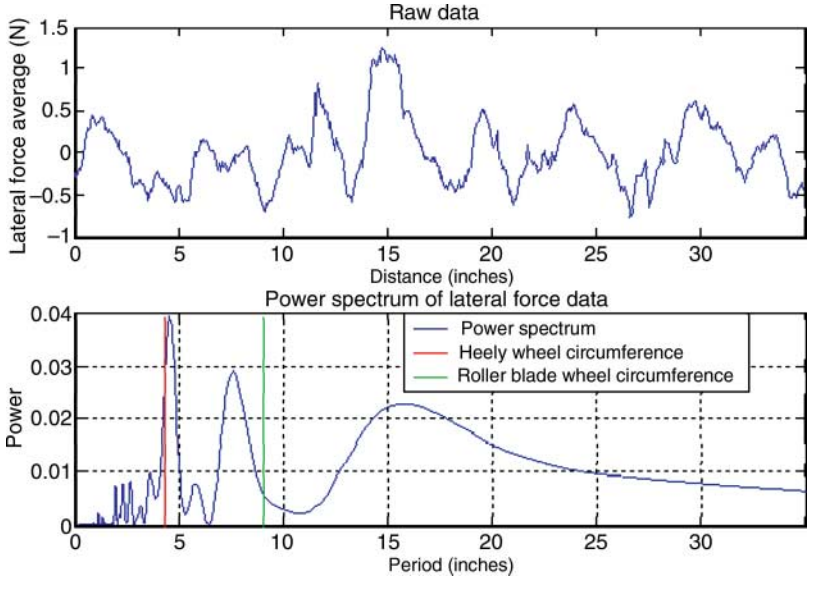

Figure 10. Fourier analysis of raw lateral force data showing signal from irregularity in the Roller shoe wheels and the inline skate wheel.

3.5. *Sources of noise*

Besides issues with the horizontal and vertical tracks, we identified several other sources of noise in the data. A fast Fourier transform of the data reveals periodic signals with periods that closely match the circumferences of the wheels that run against the vertical track and the wheel that runs against the braking surface of the rim. We replaced the original inexpensive casters with neoprene wheels on ball bearings: off-the-shelf inline skate and roller shoe wheels and bearings (Figure 10).

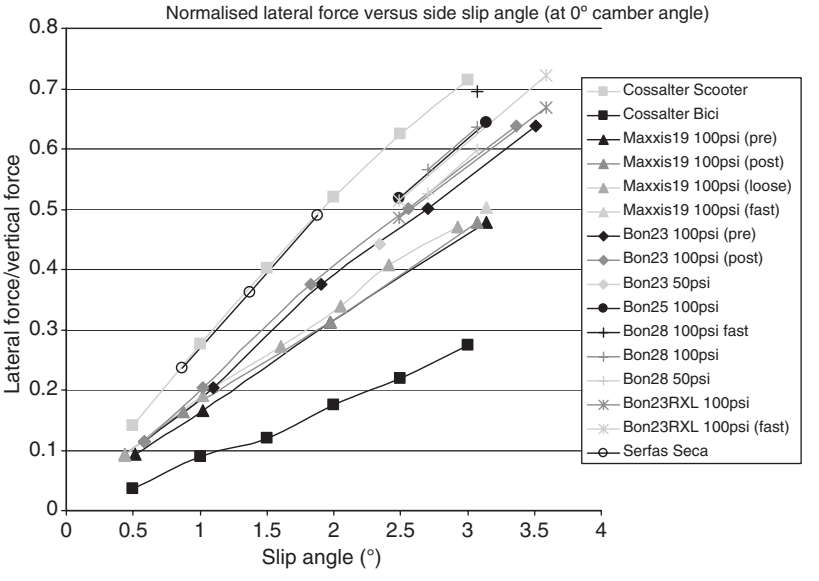

Figure 11. Normalised lateral force versus sideslip angle plotted along with data reported by Cossalter for a scooter tyre and a bicycle tyre.

4. Results

In general, the bicycle tyres tested generate a larger lateral force for a given slip angle than the bicycle tyre tested by Cossalter [1] and about the same lateral force for a given camber angle (Figure 11).

The lateral force generated in our tests by different tyres under the same camber and steer angles are easily found to vary by 10% or more: the threshold we used in the numerical simulation to determine the influence of tyre properties on the wobble mode. Thus we predict, subject to confirmation by physical testing with real tyres on real bicycles, that with the right combination of fork and wheel flexibility, changing the tyres on a bicycle may make a stable wobble unstable or vice versa.

We also find bicycle tyres to generate less than the necessary camber force so that the vector sum of ground reaction forces is in the plane of the wheel. In other words, the arctangent of the lateral force divided by the vertical load is an angle less than the camber angle. A line indicating the lateral force for which this arctangent equals the camber angle is plotted in Figure 12 and labelled 'ONE' in the legend (Figure 12).

4.1. *Radial versus bias ply*

We found the largest predictor of lateral force to be the orientation of the ply in the casing. The radial tyre, 'Maxxis', produced consistently more force for a given camber angle and less force for a given slip angle than the bias ply tyres, 'Bon'.

4.2. *Inflation pressure*

We found inflation pressure to have some effect on the lateral force with higher pressure producing a slightly higher force.

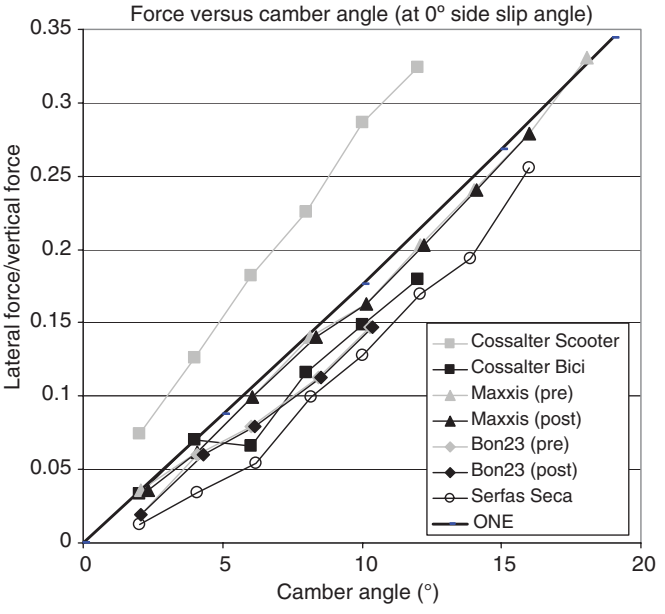

Figure 12. Normalised lateral force versus camber angle plotted along with data reported by Cossalter for a scooter tyre and a bicycle tyre.

4.3. *Tyre size*

We found tyre size, 23, 25, or 28 mm width, 'Bon23 – Bon28', for the otherwise same tyre, model, and brand, to have some effect on the lateral force with larger sizes producing a slightly higher force.

4.4. *Relaxation length*

Relaxation length is a transient property of pneumatic tyres that describes the lagging behaviour of the side force response to a sudden introduction of a slip angle [2]. It can be calculated as the ratio of cornering stiffness over the lateral stiffness [1]. It is also often calculated as the distance that a tyre rolls before the lateral force builds up to 63% of its steady-state value, preferably after having fitted the force response by an exponential function [1].

Tests on motorcycle tyres have found that the ratio of cornering stiffness over lateral stiffness produces values 20–25% higher than those calculated by the 63% method [14]. We find bicycle tyres to have a relaxation length of 4–6 cm: about 40% lower than values of 7–10 cm calculated by the 63% method.

For example, the Maxxis19 tyre, with the radial ply, generates 25 N when displaced 0.254 mm with a vertical load of 435 N and so has a lateral stiffness of 0.226 mm^{-1}. It was also measured to generate 22.5 N at a slip angle of 2° with a vertical load of 434 N and so has a cornering stiffness of 9.0 rad^{-1}. Dividing the cornering stiffness by the lateral stiffness yields a relaxation length of 40 mm. At the same time, 63% of the 22.5 N steady-state force is 14.175 N, which was observed to require 76.2 mm to accumulate.

Similarly, the Bon23RXL tyre, with bias ply, generates 48 N when displaced 0.762 mm with a vertical load of 336 N and so has a lateral stiffness of 0.188 mm^{-1}. It was also measured to generate 49 N at a slip angle of 3.6° with a vertical load of 428 N and so has a cornering stiffness of 11 rad^{-1}. Dividing the cornering stiffness by the lateral stiffness yields a relaxation

length of 59 mm. At the same time, 63% of the 49 N steady-state force is 30.87 N, which was observed to require 105 mm to accumulate.

4.5. *Self-aligning torque and twisting torque*

The torque generated in the contact patch is found to have the expected sign: the self-aligning torque, M_α in Figure 4, due to the slip angle is towards the direction of forward motion, tending to reduce the slip angle. The twisting torque, M_γ in Figure 4, due to the camber angle is towards the direction of the camber angle, tending to increase the slip angle [1,2].

4.6. *Other details*

In several cases, we measured the wheel orientation before measuring the lateral force and then again afterwards in an attempt to detect significant changes due to flexing of the cart frame. These are labelled as 'pre' and 'post', respectively, in Figures 11 and 12 In all cases, the difference was found to be very minimal.

The Serfas Seca, brand and model, respectively, the tyre was measured on an early prototype of the test device, and so its numbers are suspect. They are included here merely for completeness.

We discontinued testing of the non-zero camber angle after we discovered that the lateral force generated by bias ply tyres was not sufficient to keep the rim pressed up against the inline skate wheel and thereby allowing the camber angle to vary from the measured and recorded value.

5. Costs

Our target was to assemble the device inexpensively because the project has no outside funding. In reality, achieving that goal depended on borrowing expensive items, such as 3 m long, 1 m tall, and 30 cm wide steel I-beams, that can commonly be found in a large Civil Engineering Structures Laboratory or finding discarded items, such as various pieces of aluminium stock, in a large Engineering School machine shop.

6. Conclusions

The results show that it is not unreasonable for us to expect to find different pairs of bicycle tyres that when mounted in turn on a particular bicycle would cause the handling to be significantly different.

The test device worked well as a proof of concept, and the material and construction technique we chose enabled us to make modifications quickly and for very little additional expense. Our next design will focus on easily and reliably setting and measuring camber and steer angles to facilitate testing more tyres in less time.

References

[1] V. Cossalter, *Motorcycle Dynamics*, 2nd ed., Lulu, Raleigh, NC, 2006.
[2] H.B. Pacejka, *Tyre and Vehicle Dynamics*, Butterworth and Heinemann, Oxford, 2002.

[3] R.S. Sharp, *The stability and control of motorcycles*, Proc. IMechE C J. Mech. Eng. Sci. 13 (1971), pp. 316–329.
[4] D.G. Wilson and J. Papadopoulos, *Bicycling Science*, 3rd ed., MIT, Cambridge, MA, 2004.
[5] J.D.G. Kooijman, A.L. Schwab, and J.P. Meijaard, *Experimental validation of a model of an uncontrolled bicycle*, Multibody Syst. Dyn. 19 (2008), pp. 115–132.
[6] J.P. Meijaard, J.M. Papadopoulos, A. Ruina, and A.L. Schwab, *Linearized dynamics equations for the balance and steer of a bicycle: A benchmark and review*, Proc. R. Soc. A 463 (2007), pp. 1955–1982.
[7] V. Cossalter, G. Dalla Torre, R. Lot, and M. Massaro, *An advanced multibody model for the analysis of motorcycle dynamics*, Proceedings of the 3rd ICMEM, Beijing, China, 2009.
[8] D. Rinard, *Fork Deflection Test*, 1986. Available at http://www.sheldonbrown.com/rinard/rinard_forktest.html.
[9] A. Trovati, *Stiffness Tests*, 2008. Available at http://www.rouesartisanales.com/article-23159755.html.
[10] D.J. Cole and Y.H. Khoo, *Prediction of vehicle stability using a 'back to back' tyre test method*, Int. J. Veh. Des. 26 (2001), pp. 573–582.
[11] R.D. Roland and Massing. *A digital computer simulation of bicycle dynamics*, Tech. Rep. YA-3063-K-1, Calspan Corporation, Buffalo, NY, 1971. Prepared for Schwinn Bicycle Company.
[12] C.R. Kyle, *Gm test of tire characteristics on a flat track slow speed steel band*, Tech. Rep., General Motors, 1995. Available at http://biosport.ucdavis.edu/blog/bicycle-tire-data/.
[13] J. Bernhard, *Hands-on experiments in advanced mechanics courses*, Proceedings of the ICPE/GIREP International Conference 'Hands-on Experiments in Physics Education', Duisburg, Germany, 1998.
[14] R.T. Uil, *Non-lagging Effect of Motorcycle Tyres: An Experimental Study with the Flat Plank Tyre Tester*. Eindhoven University of Technology, Department of Mechanical Engineering, Eindhoven, The Netherlands, June 2006.